Correlated Phases of Bosons in Tilted Frustrated Lattices

Correlated phases of bosons in tilted, frustrated lattices

Susanne Pielawa, Takuya Kitagawa, Erez Berg, and Subir Sachdev
Department of Physics, Harvard University, Cambridge MA 02138
(Dated: June 6, 2011)

Abstract

We study the 'tilting' of Mott insulators of bosons into metastable states. These are described by Hamiltonians acting on resonant subspaces, and have rich possibilities for correlated phases with non-trivial entanglement of pseudospin degrees of freedom encoded in the boson density. We extend a previous study (Phys. Rev. B **66**, 075128 (2002)) of cubic lattices to a variety of lattices and tilt directions in 2 dimensions: square, decorated square, triangular, and kagome. For certain configurations three-body interactions are necessary to ensure that the energy of the effective resonant subspace is bounded from below. We find quantum phases with Ising density wave order, with superfluidity transverse to the tilt direction, and a quantum liquid state with no broken symmetry. The existence of the quantum liquids state is shown by an exact solution for a particular correlated boson model. We also find cases for which the resonant subspace is described by effective quantum dimer models.

I. INTRODUCTION

The observation of the superfluid-insulator quantum phase transition of ultracold bosonic atoms in an optical lattice[1] has launched a wide effort to engineering other correlated quantum states of trapped atoms. Much of the effort has focused on entangling the spin quantum number of the atoms between different lattice sites: superexchange interactions between neighboring lattice sites have been observed[2], but longer range spin correlations have not yet been achieved.

Here we focus on a proposal[3,4] to obtain quantum correlated phases in a pseudospin degree of freedom which measures changes in boson number across the links of a tilted lattice[6,7]. The interactions which entangle the pseudospins are not suppressed by factors of t/U (where t is the tunneling between lattice sites, and U is the local boson repulsion), and so non-trivial entanglement is likely to be readily accessible[8]. This proposal takes advantage of the unique feature of ultracold atom systems, namely, the ability to study many-body non-equilibrium physics[8,10–13], and suggests that various intriguing phases can appear as metastable states[14]. Moreover, the recent advent of site-resolved imaging of ultracold atoms in optical lattices[15–17] opens the way to the direct detection of the pseudospin and the investigation of its quantum correlations.

The previous theoretical work on tilted lattices[3–5] focused on simple cubic lattices in spatial dimensions $d = 1, 2, 3$, with the tilt along one of the principal cubic axes. In $d = 1$, this theory predicted Ising density wave order for strong tilt, and this has been observed in recent experiments[8]. Here, we will study a variety of other lattices and tilt directions. We will find analogs of the density wave and anisotropic superfluid phases found earlier. However we will also find new quantum liquid states, and some cases which map onto the quantum dimer model. These states entangle the displacements of all the atoms, and so should be attractive targets of future experiments. We will find an exact liquid ground state for a particular correlated boson model.

We begin by recalling the Hamiltonian of a tilted Mott insulator. It is described by the generalized bosonic Hubbard model[9] with an additional potential gradient along a certain direction: $H = H_{\rm kin} + H_{\rm U} + H_{\rm tilt}$:

$$H_{\rm kin} = -t \sum_{<ij>} \left(\hat{b}_i^\dagger \hat{b}_j + \hat{b}_j^\dagger \hat{b}_i \right) \tag{1.1a}$$

$$H_{\rm U} = \frac{U}{2} \sum_i \hat{n}_i (\hat{n}_i - 1) + \frac{U_3}{6} \sum_i n_i (n_i - 1)(n_i - 2) + \ldots \tag{1.1b}$$

$$H_{\rm tilt} = -E \sum_i \mathbf{e} \cdot \mathbf{r}_i \, \hat{n}_i. \tag{1.1c}$$

Here $\hat{b}_i$ are canonical boson operators on lattice sites i at spatial co-ordinate $\mathbf{r}_i$, and $\hat{n}_i \equiv \hat{b}_i^\dagger \hat{b}_i$. The first term in $H_{\rm U}$ describes two body interactions. The second term is an effective three

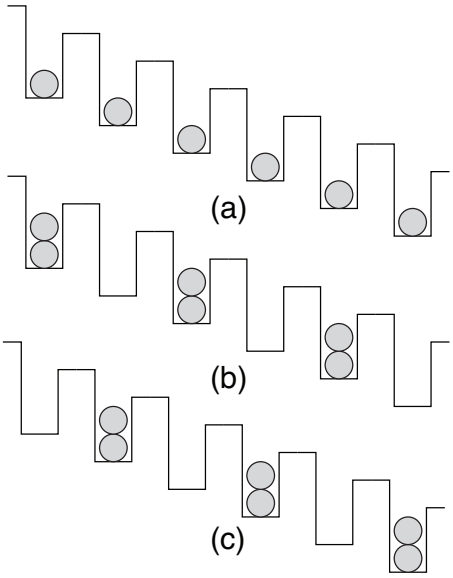

FIG. 1: (a) Parent Mott insulator, which is the ground state for $\lambda \to \infty$. (b,c) Ground states with Ising density wave order for $\lambda \to -\infty$.

body interaction, generated by virtual processes involving higher bands[18,19]. Such a term is present in ultracold atomic systems, as has recently been measured[18–20]. As we will show, the presence of this term dramatically changes the physics of tilted two dimensional lattices, therefore we include it in our model. The potential gradient is E, and the fixed vector $\mathbf{e}$ is normalized so that the smallest change in potential energy between neighboring lattice sites has magnitude E. We will assume a filling of one atom per site in the parent Mott insulator in most of the following discussion.

We are interested in the dynamics of the resonant subspace that appears when the lattice is tilted so that E becomes of order U. Specifically, we will work in the limit

$$|\Delta|, t \ll E, U, \tag{1.2}$$

where we define

$$\Delta = U - E. \tag{1.3}$$

We also define our tuning parameter

$$\lambda \equiv \frac{\Delta}{t}, \tag{1.4}$$

and allow λ to range over all real values. Thus we include processes which carry energy denominators of order $U - E$ to all orders, but neglect processes which have energy denominators of order U or E.

Let us now review the properties[3] of a tilted chain of sites in $d = 1$; see Fig. 1. As explained in Ref. 3, the limit Eq. (1.2) defines a strongly interacting many-body problem in the resonant subspace, which can be described by an effective Hamiltonian. Unlike the underlying Hubbard model in Eq. (1.1c), the energy of this effective Hamiltonian is bounded

from below, and it makes sense to study its stable ground state and low-lying excitations by the traditional methods of equilibrium many body theory. This will help us describe the dynamics of experimental studies in the metastable resonant subspace of the full Hubbard model in Eq. (1.1c) defined by Eq. (1.2). It was found that the resonant subspace was described by a quantum Ising model for an Ising pseudospin residing on the links of the chain: an up spin represented the transfer of an atom across the link (or the creation of a dipole particle-hole pair), while the down spin had no change from the parent Mott insulator. In other words, in a parent Mott insulator with occupancy n_0 per site, a down spin was a pair of sites with occupancy (n_0, n_0), while an up spin was $(n_0 - 1, n_0 + 1)$. The Ising model had both a longitudinal and transverse external field, representing the energy of the dipole and the tunneling amplitude of the atom respectively. However, two nearest neighbor dipoles cannot be created simultaneously, and this implied the presence of infinitely strong nearest-neighbor *antiferromagnetic* exchange interactions. It is this infinitely strong exchange which allows easy access to strong-correlation physics in such tilted lattices[8]. The phase diagram of the Ising antiferromagnet with both longitudinal and transverse fields has also been studied by others,[21,22] with different physical motivations. For $\lambda \to \infty$, the Ising model had a paramagnetic ground state, corresponding to configurations close to the parent Mott insulator. In contrast for $\lambda \to -\infty$, the Ising model had antiferromagnetic long-range order, corresponding to a maximum density of particle-hole pair excitations about the Mott insulator. There are two possible ways of arranging these excitations, depending upon whether the particles reside on the odd or even sites, and this ordering is linked to the antiferromagnetic order of the Ising model. In between these limit cases, a quantum phase transition was found[3] at an intermediate value of λ: this transition was in the universality class of the quantum Ising *ferromagnet* in a transverse field and zero longitudinal field[3,21,22].

Next, let us review[3] cubic lattices in dimensions $d > 1$, with a tilt along a principal lattice axis, with $|U_3| \gg t$. Then we have to distinguish the physics parallel and transverse to the tilt direction. Parallel to the tilt direction, the physics is similar to $d = 1$: there is an Ising density wave order associated with dipolar particle-hole pairs, which turns on as λ decreases. In contrast, transverse to the tilt direction, the quantum motion of individual particles and holes is allowed, not just of dipole bound states. Such motion raises the possibility of Bose condensation of particles/holes and of the appearance of superfluidity. However, the single particle or hole motion is constrained to be purely transverse. Consequently there are an infinite number of conservation laws, one for each lattice layer orthogonal to the tilt direction: the total number of particles in any layer is constrained to equal the total number of holes in the preceding layer. Because of these conservation laws, the superfluidity is not global, but restricted to each transverse layer separately: there is no Josephson tunneling term which links the superfluid order parameter of adjacent layers. Of course, because of the translational symmetry in the effective Hamiltonian parallel to the tilt, the superfluidity appears simultaneously in all the layers. In this superfluid state, atomic motion is insulating parallel to the tilt, and superfluid transverse to the tilt. Such transverse-superfluid states also

appear as λ decreases, and can co-exist with the Ising order parallel to the tilt. The previous work[3] did not note the U_3 term, even though its presence is required for the applicability of the $d > 1$ dimensional results therein.

In the present paper we will examine several tilted two dimensional lattices. We find that the physics not only depends on the lattice geometry and tilt direction, but also on the magnitude of U_3 compared to other energy scales of the systems. This U_3 term is needed to guarantee the stability of some lattices, as for example the cubic lattices reviewed above. The reason is the following. Let us assume a parent Mott insulator with filling $n_0 = 1$. Processes of the kind $(1,1) \to (0,2)$ cost repulsion energy U, and gain tilt-energy E (if the two participating sites differ in potential energy E). These processes are tuned to be resonant. Depending on the lattice structure, it may then happen that two sites differing in potential E are each occupied by two bosons. The process $(2,2) \to (1,3)$ costs repulsion energy $U + U_3$, and gains potential energy E. In the case $|U_3| \gg t$ this process is off-resonant. We can then identify a resonant subspace which focuses on the $(1,1) \to (0,2)$ processes only. This was implicitly assumed in Ref. 3 without discussion of the crucial role played by U_3, and will be assumed in our Sections II-IV. In such cases, our effective Hamiltonian[23] method applies, the energy of the resonant subspace is bounded from below, and we can use equilibrium methods to study the phase diagrams.

On the other hand, if $|U_3| \lesssim t$, we cannot neglect processes of the type $(2,2) \to (1,3)$. In the presence of such processes, the resonant Hilbert space is increased. This can have dramatic consequences on the physics; in some cases, we find that the energy in the resonant subspace becomes unbounded from below, and the system becomes unstable.

The present paper will examine several lattice configurations of Eq. (1.1c) in $d = 2$. We will assume $|U_3| \gg t$ in all cases, except in Section V. We will find analogs of the Ising and transverse-superfluid phases described above in these lattices. However, we will also find a qualitatively new phenomenon: the appearance of quantum liquid ground states with no broken symmetries. These phases appear in these lattices for two main reasons. First, even for a large tilt, not all the sites can participate in the creation of particles or holes due to the geometrical constraints present in these lattice configurations. Such geometrical constraints generate exponentially large degenerate states in the limit of infinite tilt. Secondly, the lattice structure ensures that there is no free motion of unbound particles or holes in the direction transverse to the tilt in the resonant subspace. The absence of such unbound motion prevents transverse-superfluidity, allowing for the appearance of the quantum liquid states.

The outline of the remainder of the paper is as follows. In Section II we study a square lattice with a tilt in a diagonal direction, while in Section III we study a triangular lattice with different tilt directions. In these cases, we will find analogs of phases studied previously, involving Ising density wave and transverse-superfluid order. In Section IV, we will consider the kagome and certain decorated square lattices. Here, the transverse-superfluid order is suppressed for certain tilt directions, and novel quantum liquid ground states appear. Also,

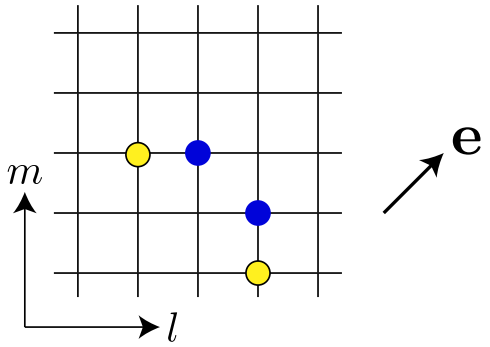

FIG. 2: (Color online) Full blue circles denote quasiparticles, and black circles with light yellow filling denote quasiholes. The tilt vector is $\mathbf{e} = (1, 1)$ and the resonant particle-hole excitations are as shown in the figure.

for another tilt direction on the kagome, the Ising density wave order is suppressed, and we obtain effective decoupled one dimensional systems. In Section V, we briefly discuss the $U_3 = 0$ case.

II. SQUARE LATTICE

As noted in Section I, this section always assumes $|U_3| \gg t$. We have already reviewed the results of Ref. 3 for a square lattice tilted along a principle lattice direction. Ref. 3 also briefly considered a tilt along a diagonal lattice direction, and we will discuss this case more completely in the present section.

For the diagonal tilt, we choose the vector $\mathbf{e} = (1, 1)$ in the Hubbard model in Eq. (1.1c). In this situation each site has two neighbors to which resonant tunneling is possible; see Fig. 2. Here and in the following, we label the lattice sites as (l, m) where l (m) represents the x (y) coordinate, respectively. Using the methods of Ref. 3, the Hamiltonian of the resonant subspace can be written as

$$H_{ph} = -t\sqrt{n_0(n_0+1)}\sum_{lm}\left[\left(\hat{p}^\dagger_{l(m+1)} + \hat{p}^\dagger_{(l+1)m}\right)\hat{h}^\dagger_{lm} + \text{H.c.}\right] + \frac{\Delta}{2}\sum_{l,m}\left(\hat{p}^\dagger_{lm}\hat{p}_{lm} + \hat{h}^\dagger_{lm}\hat{h}_{lm}\right). \tag{2.1}$$

Here we have introduced bosonic quasiparticles $\hat{p}^\dagger_{lm}$ and quasiholes $\hat{h}^\dagger_{lm}$, and we identify the parent Mott insulator with filling n_0, $|Mn_0\rangle$, as quasiparticle and quasihole vacuum, $|0\rangle$, and so

$$\hat{p}^\dagger_{l,m}|0\rangle := \frac{1}{\sqrt{n_0+1}}\hat{b}^\dagger_{l,m}|Mn_0\rangle, \tag{2.2}$$

$$\hat{h}^\dagger_{l,m}|0\rangle := \frac{1}{\sqrt{n_0}}\hat{b}_{l,m}|Mn_0\rangle. \tag{2.3}$$

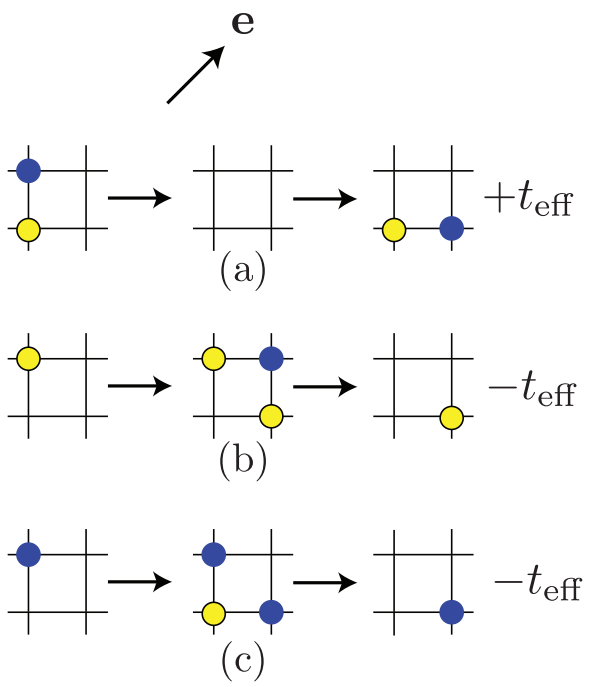

FIG. 3: (Color online) The matrix elements for the above processes are $+t_{\rm eff}$ for process (a), and $-t_{\rm eff}$ for (b) and (c).

These operators are hard-core bosons and so we have the constraints

$$\hat{p}^\dagger_{l,m}\hat{p}_{l,m} \leq 1, \tag{2.4a}$$
$$\hat{h}^\dagger_{l,m}\hat{h}_{l,m} \leq 1, \tag{2.4b}$$
$$\hat{p}^\dagger_{lm}\hat{p}_{lm}\hat{h}^\dagger_{lm}\hat{h}_{lm} = 0. \tag{2.4c}$$

We are now interested in describing the global ground state of the effective Hamiltonian in Eq. (2.1) while it is subject to the constraints in Eqs. (2.4). It is useful to first consider the limits of $\lambda \to \infty$ and $\lambda \to -\infty$, followed by a general discussion.

A. Limit $\lambda \to \infty$

To zeroth order in $1/\lambda$, the unique ground state is the vacuum, the parent Mott insulator. All particle-hole excitations are gapped with the same energy (see Fig. 2), $E_1 = \Delta$. At second order in $1/\lambda$, we obtain an effective Hamiltonian for particles and holes, whose structure is strongly constrained by Eq. (2.4). A number of distinct processes appear in the perturbation theory:

- Overall energy shift due to virtual processes. The vacuum couples to all states with one neighboring particle-hole pair, and so the vacuum energy is shifted down. Each

particle-hole state couples to zero and two particle-hole states. To second order the energy E_0 for the vacuum and E_1 for states with one particle hole pair are:

$$E_0 = -2N\frac{t^2}{\Delta}n_0(n_0+1), \tag{2.5}$$

$$E_1 = = \Delta - (2N-8)\frac{t^2}{\Delta}n_0(n_0+1). \tag{2.6}$$

where N is the number of lattice sites.

- Hopping of particles and holes along direction transverse to the tilt: Particles and holes can hop *individually* via second order processes along lines which are orthogonal to the tilt direction, see Fig. 3b,c. The magnitude of the effective hopping is

$$t_{\text{eff}} = \frac{t^2 n_0(n_0+1)}{|\Delta|}. \tag{2.7}$$

  It is this process which leads to transverse superfluidity. Of course, because the superfluidity is now one-dimensional, it is only quasi-long range, and characteristic of a Luttinger liquid.

- When particles and holes are proximate to each other, we should consider their hopping as contributing to the hopping of a dipole particle-hole pair. One such process is shown in Fig. 3a, and it leads to the motion of a particle (or rotation of a dipole) with matrix element opposite to that without an adjacent hole.

Collecting these processes, we can write down an effective Hamiltonian in the manifold of excited states with one particle hole pair (with energy $\approx \Delta$). We label $(l_p,\ m_p)$ the position of the quasiparticle, and $(l_h,\ m_h)$ the position of the hole. Clearly the vacuum state only couples to states where particle and hole are on neighboring transverse diagonals, so that $m_p + l_p = m_h + l_h + 1 = d$. We only need three integers to describe the positions of particle and hole: d, m_p, m_h. We label the states by

$$|d, m_p, m_h\rangle = \hat{p}^\dagger_{d-m_p,m_p}\hat{h}^\dagger_{d-m_h-1,m_h}|0\rangle \tag{2.8}$$

and the effective Hamiltonian in this manifold is

$$\begin{aligned} H_{\text{ph, eff}} = E_1 + t_{\text{eff}}\sum_{d,m}\Big[&\left(|d,m,m\rangle + |d,m,m-1\rangle\right)\left(\langle d+1,m,m| + \langle d+1,m+1,m|\right) \\ &+ |d,m,m\rangle\langle d,m+1,m| + |d,m,m\rangle\langle d,m,m-1| + \text{H.c.}\Big] \\ -t_{\text{eff}}\sum_{d,m_p\neq m_h}\Big[&|d,m_p,m_h\rangle\langle d,m_p+1,m_h| + |d,m_p,m_h\rangle\langle d,m_p,m_h-1| + \text{H.c.}\Big]. \end{aligned} \tag{2.9}$$

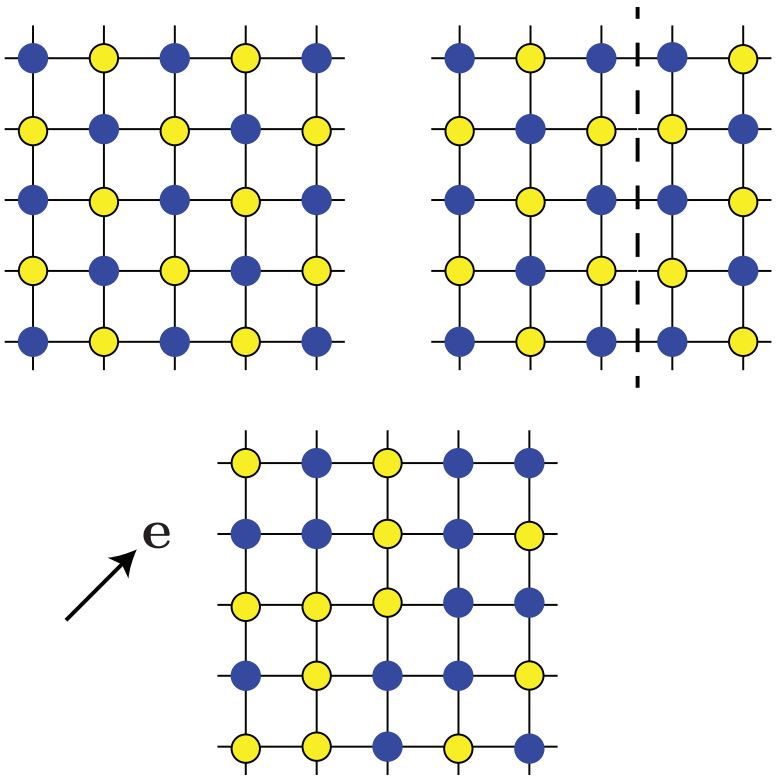

FIG. 4: (Color online) $\lambda \to -\infty$: Three possible states with maximum dipole density. At zeroth order in $1/|\lambda|$, these states are degenerate, along with an infinite number of other state with the same dipole density. At second order in $1/|\lambda|$, two states are selected as the global ground states: the checkerboard state on the top-left, and its symmetry-related partner. The state in the top-right has a domain wall between the two checkerboard states: the domain wall costs energy $t^2/(2\,|U-E|)$ per unit length.

Here the first sum is for hopping of particle-hole pairs, both in transverse and longitudinal direction of the tilt. The second sum is for particles and holes hopping individually in transverse direction. Diagonalization of this Hamiltonian, as in Ref. 3, yields a continuum of separated particle-hole excitations, along with a dipolar particle-hole bound state.

B. Limit $\lambda \to -\infty$

At zeroth order in $1/|\lambda|$ there are an infinite number of degenerate ground states, all maximizing the number of particle-hole pairs. Three such states are shown in Fig. 4. In Ref. 3, it was stated that these degenerate ground states can be labelled by the set of dimer coverings of the square lattice: this is incorrect, because given a set of particle and hole configurations, there is, in general, no unique assignment of them into nearest-neighbor dipoles.

We can examine the lifting of the ground state degeneracy in a perturbation theory in

$1/|\lambda|$. At leading order, the matrix elements in the ground state subspace are all diagonal. Each particle that has one hole to the left or below, can undergo a virtual annihilation, reducing the energy by $(t^2/|\Delta|)n_0(n_0+1) = t_{\rm eff}$. If it has two neighbors that are holes (left and below) it can do two virtual hopping processes, reducing its energy by $2t_{\rm eff}$. Thus we should optimize the latter configurations: this leads to two degenerate ground states, which look like checkerboards. These states break a lattice translation symmetry, and there is an Ising order parameter.

C. Discussion

The basic phenomenology that has emerged from our discussion so far of the diagonal tilted square lattice is quite similar to that for the principal axis tilt considered in Ref. 3. For $\lambda \to \infty$, we have continua of particle-hole excitations, while for $\lambda \to -\infty$ we have a state with Ising density wave order, and domain wall excitations. While for the principal axis tilt, these results appeared already at first order in $1/|\lambda|$, here for the diagonal tilt case we had to go to order $1/\lambda^2$ to obtain the free hopping of particles and holes, and the appearance of the Ising order. We don't expect these distinctions to be important at smaller values of $|\lambda|$, and so the phase diagram of the diagonal tilt case should be similar to that of the principal axis tilt: Ising order appearing as λ decreases, along with transverse quasi-superfluidity at intermediate values of λ.

III. TRIANGULAR LATTICE

As in Section II, this section also assumes $|U_3| \gg t$. The triangular lattice case is very similar to the square lattice case. The phase transitions are to Ising density-wave ordered states and possibly transverse quasi-superfluid phases. The tilt breaks the rotation symmetry, so the dipole states on the tilted triangular lattice are not frustrated.

A. Tilt along a principal lattice direction

For the tilt along a lattice direction, e.g. $\vec{a}_1$, we choose the tilt magnitude so that the creations of dipoles along the two other lattice directions, $\vec{a}_2$ and $\vec{a}_3$, are resonant (see Fig. 5a) but the dipole creation along the direction $\vec{a}_1$ is *not*. Therefore, the effective Hamiltonian in the resonant subspace for this case is the same as for the square lattice with a diagonal tilt, and all conclusions from Section II apply here.

One could also choose the tilt magnitude so that processes along $\vec{a}_1$ are resonant. Then all processes along $\vec{a}_2$ and $\vec{a}_3$ are off-resonant, and the resonant subspace separates into decoupled one-dimensional systems.

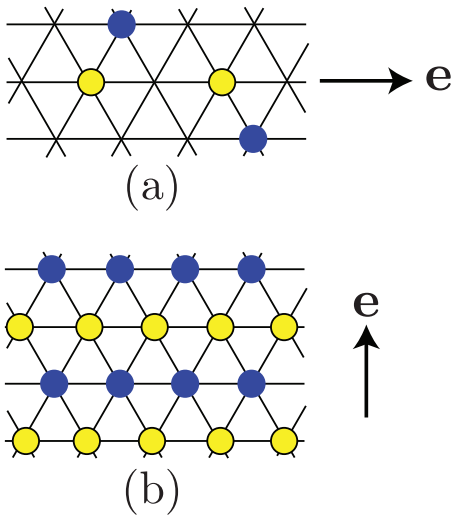

FIG. 5: (Color online) (a) Triangular lattice tilted along principal lattice direction. The effective Hamiltonian of the resonant subspace for this system is the same as the one for a square lattice with diagonal tilt. Full blue circles denote quasiparticles, and black circles with yellow filling denote quasiholes. (b) Triangular lattice tilted perpendicular to a principal lattice direction. For large negative λ, there are two-fold degenerate ground states with broken lattice symmetry.

B. Tilt perpendicular to a principal lattice direction

Here we briefly consider a triangular lattice with tilt along a principal direction. In the limit $\lambda \to \infty$, the ground state is the parent Mott insulator and all excitations are gapped. Particles and holes can separate and hop along the axis transverse to the tilt direction and reduce their kinetic energy.

On the other hand, for large and negative λ, there are precisely two degenerate ground states, as illustrated in Fig. 5b. There is an Ising density wave order parameter associated with these states. These states and their symmetries are similar to those found for the tilted square lattice in Ref. 3, and a similar phase diagram is expected.

IV. DECORATED SQUARE AND KAGOME LATTICES

As in Sections II and III, this section also assumes $|U_3| \gg t$. We will now consider frustrated models in the sense that in the strongly tilted limit, $\lambda \to -\infty$, not all sites can participate in dipole creation. This requires lattices with a larger unit cell, as will become clear from our discussion. Furthermore, the tilt direction of those lattices can be chosen such that independent motion of particles and holes is not possible in the resonant subspace. We can then label the resonant subspace by a set of dipole coverings. In the limit $\lambda \to -\infty$, we will obtain a large degeneracy in the dense dipole states. This degeneracy is lifted by corrections in inverse powers of $|\lambda|$. The leading corrections are not diagonal in the basis of dipole coverings: this sets up the possibility for novel quantum liquid phases.

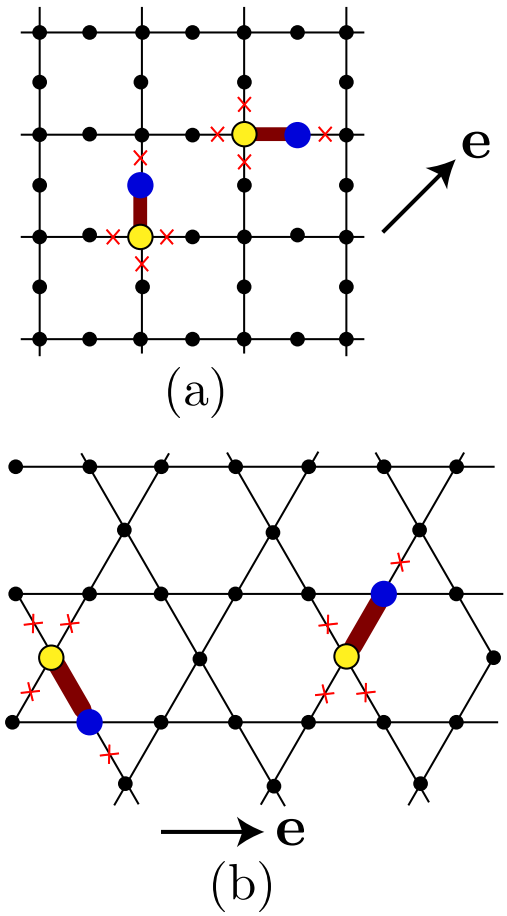

FIG. 6: (Color online) (a) Decorated square lattice in diagonal tilt, and (b) kagome lattice with tilt along lattice direction, where the tilt strength is chosen so that only processes along the diagonal lines are resonant. These two models lead to the same effective Hamiltonian in the resonant subspace. Excitations of the parent Mott insulator are dipoles (shown as think lines connecting quasiparticle and quasihole). The particles and holes cannot separate. Each dipole link blocks four other links from forming dipoles (shown as crosses). Those are also the four links onto which each dipole is allowed to hop through virtual processes.

A. Decorated square lattice with a diagonal tilt

Here we consider a decorated square lattice tilted along a diagonal direction, as illustrated in Fig. 6a. We define the distance between nearest-neighbor sites to be a so that the unit cell of the square lattice in Fig. 6a has size $2a$.

Interestingly, the effective Hamiltonian for the resonant subspace resulting from the tilted kagome lattice shown in Fig. 6b is the same as the one obtained in the decorated square lattice in Fig. 6a. While the geometry of the kagome lattice is different from the decorated square lattice, for the specific tilt of Fig. 6b, dipoles cannot be resonantly created along the links parallel to the tilt direction. This reduces the geometry of the tilted kagome to the tilted decorated square lattice. Using this identity, we will present most of the results using

the decorated square lattice illustrated in Fig. 6a.

The decorated square lattice has 3 sites per unit cell. Let N be the number of unit cells, and we assume periodic boundary conditions. There are two kinds of sites on this lattice: N sites that have four neighbors, and $2N$ sites that only have two neighbors. We define the unit cell so that a site with four neighbors is in its center. We will refer to these sites as central sites.

The Hamiltonian in the resonant subspace is

$$H = \Delta \sum_a \hat{d}_a^\dagger \hat{d}_a - t\sqrt{n_0(n_0+1)} \sum_a \left(\hat{d}_a + \hat{d}_a^\dagger \right),$$

where a labels the lattice links, and $\hat{d}_a^\dagger$ creates a dipole on this link. The resonant subspace has the constraints

$$\hat{d}_a^\dagger \hat{d}_a \leq 1, \tag{4.1}$$

and

$$\hat{d}_a^\dagger \hat{d}_a \hat{d}_{a'}^\dagger \hat{d}_{a'} = 0 \tag{4.2}$$

if a and a' share a lattice site, see Fig. 6. Note that particles and holes cannot separate on this lattice through hopping in the resonant subspace. It is notable that this effective model restores the rotational symmetry of the lattice and is symmetric under rotation of $\pi/2$ around the central sites.

1. *Limit $\lambda \to \infty$*

Here the ground state is the parent Mott insulating state. The excitations are gapped and the lowest excitations are given by the creation of a single dipole. To zeroth order in $1/\lambda$, all states with one dipole are degenerate. We now describe the effective Hamiltonian for the manifold of excited states with energy $\approx \Delta$ to second order in $1/\lambda$. First of all, there are energy shifts for the vacuum energy E_0 and energy of one dipole E_1, given by

$$E_0 = -4N t_{\text{eff}} \tag{4.3}$$

$$E_1 = \Delta - (4N-6) t_{\text{eff}} \tag{4.4}$$

with

$$t_{\text{eff}} = \frac{t^2 n_0(n_0+1)}{|\Delta|}. \tag{4.5}$$

Additionally, second order processes lead to hopping of the dipoles. Note that a dipole always involves one central site and one neighboring site located to the right, left, up or down relative to the central site. Thus, we label the dipole states by $|l, m, \sigma\rangle$, where (l, m) denotes the position of the central site and $\sigma = 1, 2, 3, 4$ indicates the direction of the dipole,

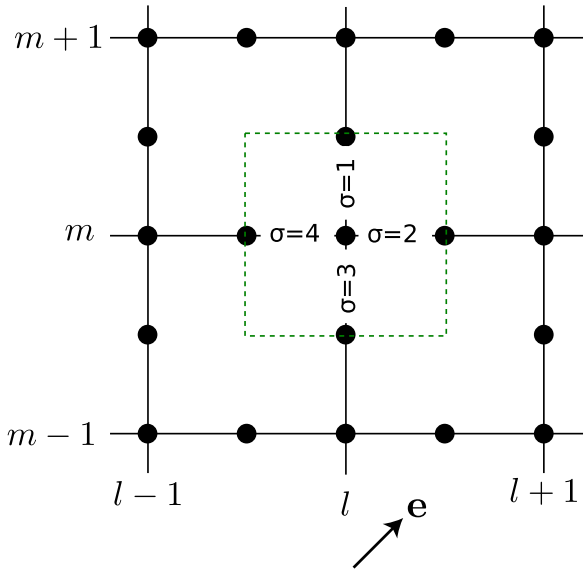

FIG. 7: (Color online) Labeling of sites and links on the decorated square lattice.

see Fig. 7. With this notation, the effective Hamiltonian for one dipole excitation is given by

$$\begin{aligned} H_{\text{1dimer}} &= E_1 + t_{\text{eff}} \sum_{\sigma\neq\sigma',m,l} |l,m,\sigma\rangle \langle l,m,\sigma'| \\ &\quad + t_{\text{eff}} \sum_{l,m} \left[|l,m,1\rangle \langle l,m+1,3| + |l,m,2\rangle \langle l+1,m,4| + \text{H.c.} \right]. \end{aligned} \tag{4.6}$$

The first sum represents hopping of the dipole at a central site from one orientation to another, and the second sum represents hopping from one unit cell to another. Diagonalizing the above Hamiltonian Eq. (4.6), one obtains the spectra of a single dipole excitation given by

$$\epsilon_1(k_x,k_y) = E_1 - 2t_{\text{eff}} \tag{4.7}$$

$$\epsilon_2(k_x,k_y) = E_1 \tag{4.8}$$

$$\epsilon_3(k_x,k_y) = E_1 + \left(1 - \sqrt{5 + 2\cos(2ak_x) + 2\cos(2ak_y)}\right) t_{\text{eff}} \tag{4.9}$$

$$\epsilon_4(k_x,k_y) = E_1 + \left(1 + \sqrt{5 + 2\cos(2ak_x) + 2\cos(2ak_y)}\right) t_{\text{eff}} \tag{4.10}$$

where $2a$ is the distance between two neighboring central sites. The first two bands are 'flat bands' as they do not depend on momentum.

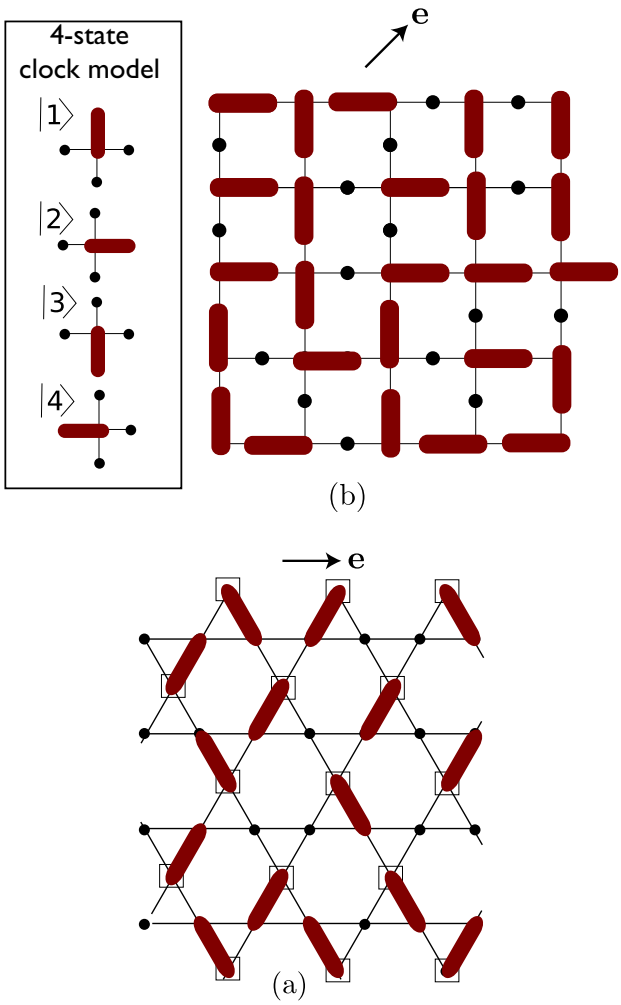

FIG. 8: (Color online) $\lambda \to -\infty$: quantum 4-state clock model: (a) decorated square lattice, (b) kagome lattice. Both lattices lead to the same effective Hamiltonian. Minimum of the energy for the effective Hamiltonian is obtained when the number of dipoles is maximum. This requires, on the square lattice, every central site to have a dipole, and on the kagome lattice, every site marked with a square to have a dipole. As a result, we can look at the system in the limit $\lambda \to -\infty$ as a collection of four state clocks, one each on the central sites of the square lattice, or on the marked sites of the kagome. The states on neighboring clocks are constrained by the requirement that the dipoles cannot overlap.

2. Limit $\lambda \to -\infty$, quantum liquid state

To zeroth order in $1/\lambda$, all states which maximize the number of dipoles are degenerate, and they are all ground states of the effective Hamiltonian. These states require every central site on the square lattice to have a dipole (on the kagome lattice, every site marked with a square has a dipole), as illustrated in Fig. 8. There is an exponentially large number of such states which satisfy this requirement.

To second order in $1/|\lambda|$, dipoles can hop as long as the constraint Eq. (4.2) is satisfied.

As there is a dipole on every central site, the constraint implies that dipoles may only change their orientation while remaining at the same central site. Thus, we can write the hopping of the dipoles as a 4-state quantum clock model, with the clocks residing on the vertices of the square lattice. The hopping Hamiltonian can be written as (see Fig. 8)

$$\begin{aligned} H_{\text{clock}} &= \sum_{lm} H_{l,m} \\ H_{l,m} &= \Delta - t_{\text{eff}}(|1\rangle + |2\rangle + |3\rangle + |4\rangle)(\langle 1| + \langle 2| + \langle 3| + \langle 4|) \end{aligned} \tag{4.11}$$

where (l, m) is the site index, and $|\sigma\rangle$ is a shorthand for $|l, m, \sigma\rangle$ representing the orientation of the dipole sitting at (l, m). It should be remembered that states within the resonant subspace have the important constraint that two dipoles sitting at neighboring central sites cannot be directed toward each other. Such constraints are not contained in H_{clock}. If we define the projection operator onto the resonant subspace which satisfies the constraints as P, the effective Hamiltonian with the constraints is given by projecting the hopping Hamiltonian,

$$H^c_{\text{clock}} = P H_{\text{clock}} P. \tag{4.12}$$

In the following we will show that the *exact* ground state of the Hamiltonian with constraint H^c_{clock} is obtained through the projection of the ground state of the Hamiltonian without constraint, H_{clock}, onto the resonant subspace which satisfy the constraints Eq.(4.1). The ground state of the unconstraint single-site Hamiltonian $H_{l,m}$ is given by $|1\rangle + |2\rangle + |3\rangle + |4\rangle$ with eigenenergy $\Delta - 4t_{\text{eff}}$, and there are three degenerate excited states[1] with eigenenergy Δ. Therefore, the ground state of H_{clock} is given by

$$|\psi_0\rangle = \mathcal{N} \prod_{l,m} (|l, m, 1\rangle + |l, m, 2\rangle + |l, m, 3\rangle + |l, m, 4\rangle) \tag{4.13}$$

where $\mathcal{N}$ is some normalization constant. As we will show in the following, the exact ground state of H^c_{clock} is given by

$$|\psi_c\rangle = P\,|\psi_0\rangle\,. \tag{4.14}$$

Any configuration with maximum number of dipoles corresponds to a product state given by $\prod_{l,m} |l, m, \sigma_{l,m}\rangle$ where $\sigma_{l,m} = 1, 2, 3, 4$. Then the state $|\psi_c\rangle$ is nothing but the equal superposition of all the product states in the resonance subspace in the limit $\lambda \to -\infty$ i.e. all the configurations with maximum number of dipoles.

The proof proceeds in two steps. First, we will show that this nodeless state $|\psi_c\rangle$ is an

[1] Interestingly, it is possible to fill the lattice with these excited states while respecting the constraint: some of the highest energy eigenstates of H_{clock} are also eigenstates of H^c_{clock}. Note that states of the form $|\sigma\rangle - |\sigma'\rangle$, with $\sigma \neq \sigma'$, are excited eigenstates of the single site Hamiltonian (4.11). These states only occupy two links. We could, for example, fill the lattice with the state $|1\rangle - |2\rangle$ on every site.

eigenstate of the Hamiltonian H^c_{clock}. Second, we will show that it is necessarily the unique ground state of the Hamiltonian H^c_{clock}.

In order to see that $|\psi_c\rangle$ is an eigenstate of H^c_{clock}, we check that $H^c_{\text{clock}}|\psi_c\rangle$ is again the equal superposition of all the configurations with maximum number of dipoles. Consider a particular configuration with maximum number of dipoles represented by the product state $|M\rangle$. We count how many different configurations in $|\psi_c\rangle$ produce $|M\rangle$ after the action of H^c_{clock}. This is equivalent to counting how many different state can be created from $|M\rangle$ through the action of H^c_{clock}. For any $|M\rangle$, there are in total $2N$ different configurations that are connected with $|M\rangle$ through an action of H^c_{clock}, where N is the total number of dipoles in the system. The decorated square lattice has in total $2N$ non-central sites, and in a configuration with maximum number of dipoles $|M\rangle$, N of them are part of a dipole and N of them are *not*. Now the action of H^c_{clock} is a change of the orientation of a dipole at a central site, and the action can change the configuration by hopping a dipole to these non-central sites that are not occupied by a dipole in $|M\rangle$. Since each unoccupied non-central site is connected with 2 central sites, there are in total $2N$ different configurations connected with $|M\rangle$. This consideration is true for any $|M\rangle$, so we conclude that $H^c_{\text{clock}}|\psi_c\rangle = N(\Delta - 3t_{\text{eff}})|\psi_c\rangle$. Notice that the Hamiltonian Eq. (4.11) contains terms which bring a configuration back to itself, so the eigenenergy is $N(\Delta - 3t_{\text{eff}})$. Indeed $|\psi_c\rangle$ is an eigenstate.

Now we show that this state is necessarily the unique ground state. Note that if we take as the basis the product states which correspond to configurations with maximum number of dipoles, all the off-diagonal matrix element of H^c_{clock} are negative. Moreover, repeated applications of H^c_{clock} can connect any configuration with maximum number of dipoles to any other configurations with maximum number of dipoles. This statement is even true when the system is placed on a manifold with non-trivial topology, such as a torus. From these two conditions, it follows through Perron-Frobenius theorem[25–27] that the ground state of the effective Hamiltonian Eq. (4.11) is the superposition of product states with strictly positive amplitudes. Moreover, since two of such states cannot be orthogonal to each other, this ground state is unique. Now since we found the state $|\psi_c\rangle$ which is a superposition of product states with strictly positive amplitudes, it follows that $|\psi_c\rangle$ must be the unique ground state of the Hamiltonian.

In order to probe the properties of the ground state $|\psi_c\rangle$, we numerically computed correlations for the state in Eq. (4.14). For the correlations of local operators in a state which is the equal superposition of product states, the correlations can be related to the corresponding classical problem[24]. Here we study the density-density correlation $\langle \hat{n}_{0,0}\hat{n}_{0,m}\rangle$ on the central sites. $n_{l,m}$ is the density of the central site at (l,m) measured relative to the density of the Mott insulator, so that $n_{l,m}$ can, in principle, take the values $+1, 0, -1$. Here $+1$ (-1) means that there is an extra (a missing) boson on that lattice site, and that this site has formed a dipole with a neighbor below or to the left (above or to the right). $n_{l,m} = 0$ would mean that this central site is not participating in a dipole bond; in the

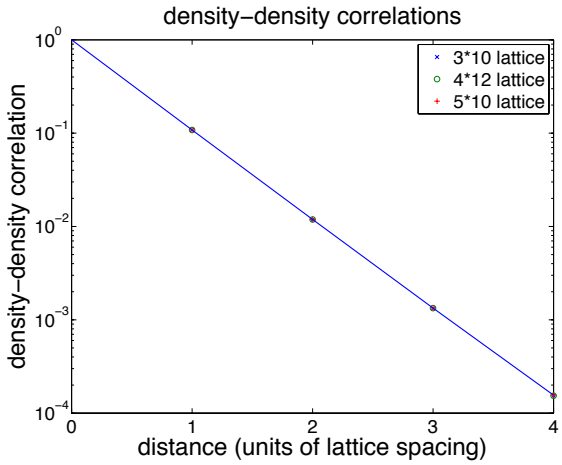

FIG. 9: (Color online) Density-density correlation function $\langle \hat{n}_{0,0}\hat{n}_{0,m}\rangle$ on the central sites (the ones marked by a square in Fig. 8), obtained using transfer matrices and periodic boundary conditions. Correlations decay rapidly in an exponential fashion. A fit to the exponential $f(m) = a\exp(-bm)+c$ gives $a = 0.9999$, $b = 2.225$, $c = 7.371\times10^{-5}$, this corresponds to a correlation length of less than half a lattice spacing.

limit $\lambda \to -\infty$ all central sites have $n_{l,m} = \pm 1$. We used row-to-row transfer matrices with rows of length up to 5 unit cells and periodic boundary conditions to compute density-density correlations[29]. Results for lattice sizes 3×10, 4×12, and 5×10 are plotted in Fig. 9. We obtain essentially the same results for different lattice sizes, and a fit of the correlation function to the exponential $f(m) = a\exp(-bm)+c$ gives $a = 0.9999$, $b = 2.225$, $c = 7.371\times10^{-5}$, corresponding to a correlation length of less than half a lattice spacing. Similarly, dipole-dipole correlations can also be calculated: let $\hat{d}_{\sigma,l,m}$ be an operator that projects onto states which have dipole orientation σ at site (l,m). We find that correlations $\langle \hat{d}_{\sigma,0,0}\hat{d}_{\sigma',l,m}\rangle - \langle \hat{d}_{\sigma,0,0}\rangle\langle \hat{d}_{\sigma',l,m}\rangle$ decay exponentially.

The exponential decay of the equal-time correlations suggests that the $\lambda \to -\infty$ liquid state has a gap to all excitations. Furthermore this liquid state is non-degenerate on a torus, implying the absence of topological order, and we expect the ground state to remain unique in the thermodynamic limit $N \to \infty$. Thus there is a possibility that the parent Mott insulator state at $\lambda \to \infty$ is adiabatically connected to the liquid state at $\lambda \to -\infty$, without an intervening quantum phase transition.

Ultracold atom experiments are expected to realize this quantum liquid state as long as the temperature is lower than the energy scale of $t_{\text{eff}} \propto t^2/|E-U|$. Since the magnitude of t_{eff} can be controlled by changing the tilting strength E, it is likely that the temperature of the order of t_{eff} is achievable in experiments. Moreover, recent experiments by Bakr *et. al.*[16] showed that the Mott phase contains particularly low entropy compared to the surrounding superfluid, and fits with theoretical curve suggest that the Mott phase is as low temperature as a few nK. Therefore, together with the demonstration of lattice tilting[1,8] and possibility to create various lattice structures through a holographic mask technique[15], realization of

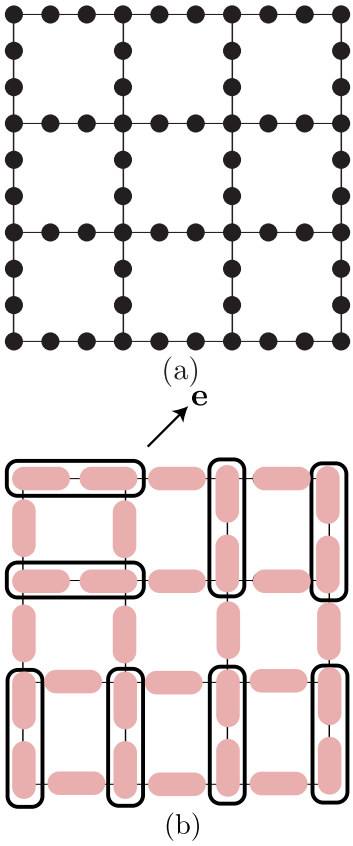

FIG. 10: (Color online) (a) The doubly-decorated square lattice. (b) Dense dipole configuration obtain in the limit $\lambda \to -\infty$. Each dipole is represented by the thick line, and consists of a particle-hole pair. Links with two dipoles are identified as having a "dimer", and these are indicated by the ovals. These dimers are described by an effective quantum dimer model.

this quantum liquid state should be possible with current technology.

B. Doubly-decorated square lattice

Although the quantum liquid state found in Section IV A has non-trivial entanglement, it does not have topological order. Here we show that by decorating the square lattice further, it is possible to obtain a model whose resonant subspace is labeled by the set of dimer packings of the undecorated square lattice. The dipole hopping terms appear in the perturbation theory of $1/\lambda$, and the effective Hamiltonian in this resonant subspace is expected to take a version of the quantum dimer model[24].

In this model, we consider a square lattice decorated by *two* sites at each link between lattice sites, as shown in Fig. 10a. Quantum spin models on a similar decorated square lattice were considered in Ref. 28. In the limit $\lambda \to -\infty$, the ground states in the resonant subspace are those with maximum number of dipoles. As before, there are a large number

of such states and they are all degenerate in this limit. The dipoles now come in two flavors: those which have one end on a central site of the square lattice, and those which reside exclusively on a link between central sites. Along a link between two central sites, the first kind of dipoles always come in pairs. We associate this pair with a "dimer" which connects two neighboring central sites (see Fig. 10b). Because there can be only one dimer on each site for $\lambda \to -\infty$, the dimers are close-packed, and there is a one-to-one correspondence between the degenerate ground state manifold and the set of dimer packings of the square lattice. Including corrections in powers of $1/|\lambda|$ we expect an effective Hamiltonian which acts on a Hilbert space of states labeled by the dimer coverings: this must have the form of the quantum dimer model[24]. In particular, a plaquette-flip term appears at order $1/|\lambda|^{12}$; up to this order, all diagonal terms in the basis of dipole coverings are equal and independent of the configurations. We leave the details of the calculations as well as possible extensions to a future work, and give a general discussion below.

On the square lattice, quantum dimer models are generically expected to have ground states with valence bond solid orders[30]. At critical points between different solid orders, topologically ordered spin-liquids can be obtained[31,32]. The quantum dimer model realized in this system consists of only a kinetic term, and no energy cost or gain for parallel dimers,

$$H_{\text{dimer}} = -t_{\text{dimer}} \sum_{\text{plaquettes}} \left(|||\rangle \langle =| + |=\rangle \langle |||\right). \tag{4.15}$$

This model is not critical, and so valence bond order is expected, but the precise nature of the square lattice symmetry breaking remains under study. An early exact diagonalization study[33] suggested a plaquette phase, more recent quantum Monte Carlo calculations[34] predicted a columnar phase, and recently a mixed columnar-plaquette phase has been proposed[35]. As λ increases away from $\lambda = -\infty$, configurations with less number of dipoles become energetically favorable. These states are analogous to those in the doped quantum dimer model[24,36], where other novel phases are possible[37]. As the parent Mott insulator at $\lambda = \infty$ is non-degenerate, it cannot be connected adiabatically to all the possible $\lambda \to -\infty$ states with topological order or broken symmetry: there must be at least one intervening quantum phase transition.

C. Kagome lattice tilted perpendicular to a principal lattice axis

At last, we study the kagome lattice tilted perpendicular to a principle axis, as illustrated in Fig. 11. Because of the low connectivity in the lattice structure, dipole creations are frustrated in the limit $\lambda \to -\infty$ and even in this limit, some sites cannot not participate in the creation of dipoles. As a result, there is no Ising ordering and the transverse superfluidity persists in the limit $\lambda \to -\infty$, as we describe below.

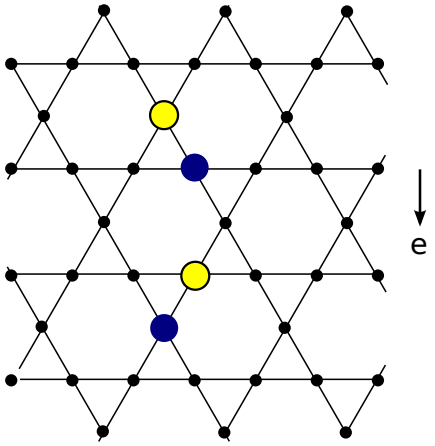

FIG. 11: (Color online) Kagome lattice tilted perpendicular to a principal lattice axis: resonant particle-hole excitations are illustrated. After a particle-hole pair is created, either the particle or the hole can hop along the direction transverse to the tilt.

1. *Limit* $\lambda \to \infty$

The ground state is again the Mott insulator, and the excitations are particles and holes. For every particle-hole pair, either the particle or the hole is located on a transverse layer where it can hop, while the other is fixed and cannot move, see Fig. 11. The dispersion of the hopping quasiholes is

$$\epsilon_h(k) = \Delta - 2n_0 t \cos(ka),$$

while for hopping quasiparticles it is

$$\epsilon_p(k) = \Delta - 2(n_0 + 1) t \cos(ka).$$

Therefore, the hopping quasiparticles have lower energy than the hopping quasiholes. The excitations are gapped for $\lambda \to \infty$, but excitations become gapless for some critical value λ_c.

2. *Limit* $\lambda \to -\infty$

The ground state in the resonant subspace has the maximum number of dipoles. Due to the geometry of the kagome lattice, some sites are frustrated in the sense that they cannot participate in the creations of dipoles. These sites allow the particles and holes to move along the horizontal direction perpendicular to the tilt, forming Luttinger liquids. As the kinetic energy of quasiparticles is lower than that of the quasiholes, the ground state maximizes the number of moving quasiparticles in a transverse layer and localizes all the quasiholes, as shown in Fig. 12. Each transverse layer thus realizes a "Tonks-Girardeau gas" of bosons at half-filling[38], and the ground state realizes a collection of uncoupled gapless Luttinger

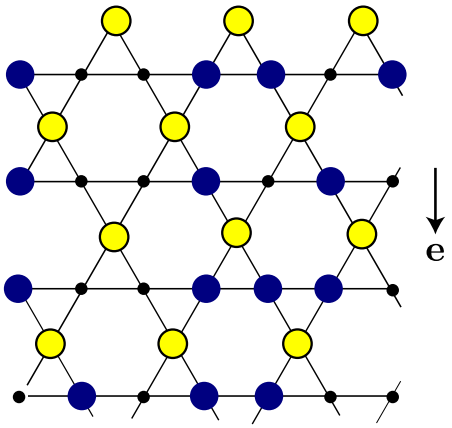

FIG. 12: (Color online) $\lambda \to -\infty$. Single non-degenerate ground state with half-filled Tonks gases along horizontal lines for $\lambda = -\infty$.

liquids. These are gapless only in the limit $\lambda = -\infty$. Perturbation theory to second order in $1/\lambda$ generates a dimerized hopping term, *i.e.* the effective hopping between two sites in a one-dimensional chain which share a neighbor above them becomes different from the hopping between sites which share a neighbor below. This breaks the translation symmetry along the one-dimensional layers explicitly, doubles the unit cell, and opens a gap, as the Tonks gases are exactly at half filling. Therefore, to order $1/\lambda^2$ the one-dimensional systems remain decoupled, but they are no longer gapless.

V. MODIFICATIONS FOR $|U_3| \ll t$

In this section we briefly discuss how the physics of tilted lattices is modified if the U_3 term in Eq. (1.1c) vanishes. In this case all processes $(n, n) \to (n-1, n+1)$ for general n are resonant at the same tilt magnitude. This greatly increases the size of space of states resonantly connected to the parent Mott insulator. As we will show in some cases the energy of this enlarged space is not bounded from below, and we then cannot use equilibrium methods to describe the physics. In other cases the resonant subspace remains bounded from below, but the phases differ from the ones found for $|U_3| \gg t$. We will illustrate this by two examples: square lattice tilted along a principle lattice direction, and diagonally tilted decorated square. We leave a more complete discussion for future study.

A. Square lattice tilted along a principal lattice direction

This case was considered in Ref. 3. However, the results there apply only if the resonant subspace is limited by a large $|U_3|$. For small $|U_3|$ the physics is quite different, as we now describe.

In particular, we can no longer use equilibrium methods, as the energy of the subspace resonantly connected to the parent Mott insulator is not bounded from below, when $\lambda \to -\infty$. Once a particle-hole pair is created, the particle and hole are each free to move in the direction transverse to the tilt. It is then possible that two quasiparticles are adjacent to each other, in such a way that they can undergo a resonant transition. The system can resonantly reach states with an arbitrarily large number of bosons on a lattice site, as illustrated in Fig. 13, leading to an arbitrarily large negative energy.

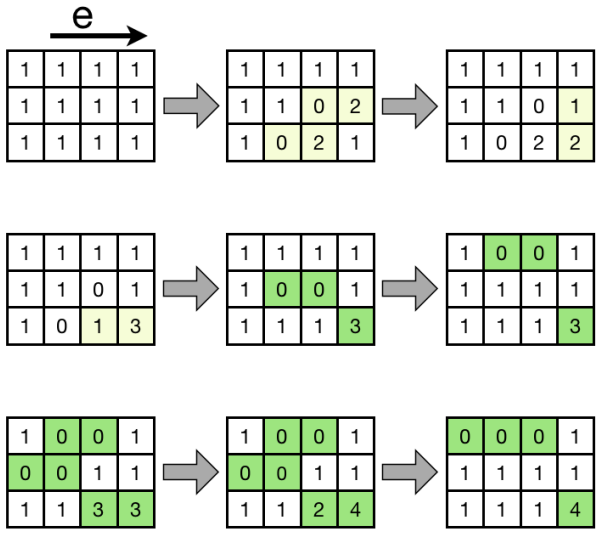

FIG. 13: (Color online) Square lattice tilted along a lattice direction for $U_3 = 0$. The number in each square represents the number of bosons at that site. Here the occupancy of the parent Mott insulator is $n_0 = 1$. We illustrate resonant processes which eventually lead to the creation of lattice sites occupied by 4 bosons. It is possible to continue this pattern, thus we obtain any arbitrarily large number n_B of bosons on a single site, through resonant processes. In the end, only a total number of n_B lattice sites remain changed (shown in green). Having n_B bosons on a site reduces potential energy $n_B(n_B-1)\Delta/2$. One could fill the lattice with such patterns. Thus the energy of states resonantly connected to the parent Mott insulator is not bounded from below.

B. Diagonally tilted decorated square lattice

This lattice remains stable: the energy of the enlarged resonant subspace is bounded from below. This stability is related to the lower connectivity of the lattice structure, and the suppression of transverse superfluidity in Section IV A. Let us consider the phases in the limit $\lambda \to -\infty$. We distinguish two cases: filling factor $n_0 = 1$, and filling factor $n_0 > 1$.

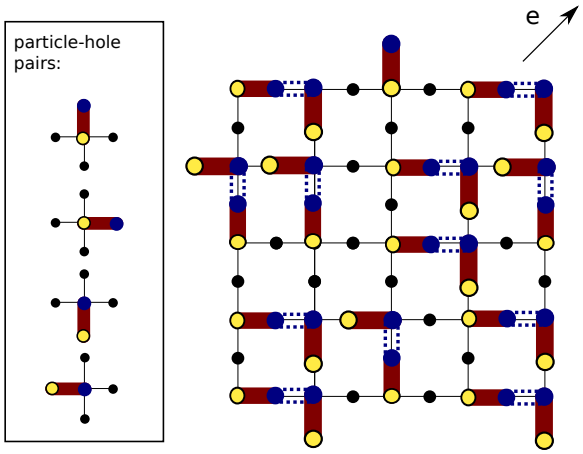

FIG. 14: (Color online) Decorated square lattice in diagonal tilt, filling factor $n_0 = 1$, $U_3 = 0$. Quasiparticles are shown as dark blue circles, quasiholes as circles with yellow filling. Two neighboring quasiparticles can form another dipole bond $(2,2) \to (1,3)$ which reduces the energy by Δ. This is indicated in the figure by dotted blue lines. Quasiholes contain no bosons, and they cannot form another dipole bond. To minimize its energy, the system not only maximizes the number of dipoles on the lattice, but also maximize the number of neighboring quasiparticles. The set of states fulfilling these requirements maps to the dimer coverings of a square lattice, and one such dimer covering is shown above.

1. *Filling of parent Mott insulator:* $n_0 = 1$

Particle-hole pairs each reduce potential energy by Δ, and they may be arranged in such a way that each quasiparticle is adjacent to another quasiparticle. This allows for a third resonant transition, $(2,2) \to (1,3)$, which again reduces potential energy by Δ. As illustrated in Fig. 14, this always leads to a central site being occupied by three bosons. Two such sites are never adjacent to each other, so that an occupation number of four or more bosons on any site cannot be reached resonantly. The energy remains bounded from below. In the limit $\lambda \to -\infty$ the resonantly connected subspace has a large number of ground states, and there is a one-to-one correspondence between this degenerate ground state manifold and the set of dimer packings on the square lattice. A plaquette-flip term of the dimers appears in order $1/\lambda^{12}$. Thus we obtain a remarkable mapping of the effective Hamiltonian to the quantum dimer model. Unlike the large U_3 case in Section IV, here the dimer model appears already for the singly-decorated square lattice, and so should be easier to realize experimentally.

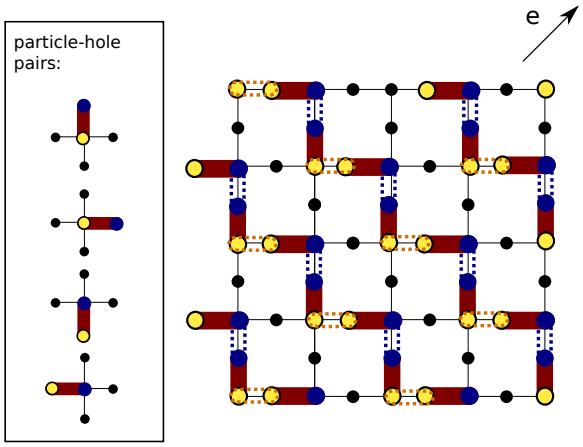

FIG. 15: (Color online) Decorated square lattice in diagonal tilt, filling factor $n_0 > 1$, $U_3 = 0$. In this case 'quasiholes' can also undergo a resonant transition, which is shown as orange dotted lines. There are two degenerate ground states with density-wave order: the one shown in the figure, and its symmetry related partner.

2. Filling of parent Mott insulator: $n_0 > 1$

If the filling factor is two or larger, then two adjacent 'quasiholes' can undergo a resonant transition $(n_0 - 1, n_0 - 1) \to (n_0 - 2, n_0)$, reducing the potential energy by Δ. Potential energy is minimized if each 'quasihole' and each 'quasiparticle' can undergo such a transition, as illustrated in Fig. 15. This leads to a two fold degenerate ground state with density-wave order: all central sites are occupied by either $(n_0 + 2)$ or $(n_0 - 2)$ bosons, while all other sites contain n_0 bosons.

VI. CONCLUSIONS

This paper has shown that there are rich possibilities for generating non-trivial quantum states upon tilting a Mott insulator of bosons. Our classical intuition tells us that applying a strong tilt to a Mott insulator should lead to a runaway instability of particles flowing downhill. However, quantum mechanically, for a single band model in the absence of external dissipation, and with a significant three-body interaction U_3, this does not happen. Instead particle motion is localized in the direction of the tilt, and free motion is only possible in orthogonal directions. It is useful to introduce the idea of a resonant subspace of states which are strongly coupled to the parent Mott insulator when the tilt approaches its critical value. Within this resonant subspace, we can define an effective Hamiltonian whose energy is bounded from below, and which has well defined equilibrium quantum phases and phase transitions. We presented a variety of such effective models here, and described general aspects of their phase diagrams. As in the previous work[3], we found phases with Ising

density wave order along the tilt direction, and superfluid/Luttinger liquid behavior in the direction transverse to the tilt. More interestingly, we showed that on a variety of frustrated or decorated lattices, particle motion can be suppressed also in directions transverse to the tilt. Then, the tilted lattices map onto quantum clock or dimer models, with novel quantum liquid and solid phases.

We also briefly noted, in Section V, the situation when $|U_3|$ was small. In some cases, the energy of the resonant subspace is unbounded from below, and so non-equilibrium methods will be necessary to understand the physics. However, for the simple case of the decorated square lattice, we found a mapping of the effective Hamiltonian to that of the quantum dimer model in a limiting case, as illustrated in Fig. 14.

It is clear that the models studied here have extensions to numerous other lattices and decorations, and that there are many promising avenues for obtaining exotic phases. It would also be interesting to study the analogous models of fermions, which could display metallic states associated with motion in the transverse directions. In principle, all these models should be readily accessible in experiments on trapped ultracold atoms.

Acknowledgments

We thank Waseem Bakr, Markus Greiner, Liza Huijse, and Jonathan Simon for many stimulating discussions. We would like to thank Fabian Essler for pointing out that the decoupled one dimensional systems in Section IV C 2 are Luttinger liquids only for λ strictly $-\infty$. This research was supported by the National Science Foundation under grant DMR-0757145, by a MURI grant from AFOSR, NSF grant DMR-0705472, DMR-090647, AFOSR Quantum Simulation MURI, AFOSR MURI on Ultracold Molecules, DARPA OLE program and Harvard-MIT CUA. S.P. acknowledges support from the Studienstiftung des Deutschen Volkes.

Appendix A: Decorated square lattice in the $\lambda \to -\infty$ limit

1. Ground state correlation functions

To calculate correlation functions in the exact ground state of the effective clock model, Eq. (4.14), we make use of the following "transfer matrix" method. For an equal-amplitude ground state, correlations of operators, $\hat{O}$, which are diagonal in the basis of dipole coverings, can be related to a corresponding classical problem

$$\langle \hat{O} \rangle = \frac{\langle \psi_c | \hat{O} | \psi_c \rangle}{\langle \psi_c | \psi_c \rangle} = \frac{\sum_M \langle M | \hat{O} | M \rangle}{D_c}. \tag{A1}$$

Here, the sum over M runs over all states that maximize the number of dipoles and respect constraints Eq. (4.1) and (4.2). We assume that all the states $|M\rangle$ are properly normalized, $\langle M|M\rangle = 1$, and define $D_c = \sum_M \langle M|M\rangle = \dim(H_c)$ as the dimension of the Hilbert space with constraint. The density operator $\hat{n}_{l,m}$ measuring the relative density at central site (l, m) is diagonal in the basis of dipole coverings; it has eigenvalues ± 1. Therefore, $\langle \hat{n}_{(0,0)} \hat{n}_{(l,m)} \rangle$ can be written as

$$\langle \hat{n}_{(0,0)} \hat{n}_{(l,m)} \rangle = \frac{N_+ - N_-}{D_c}, \tag{A2}$$

where $N_\pm$ is the number of configurations which have $\langle M| \hat{n}_{(0,0)} \hat{n}_{(l,m)} |M\rangle = \pm 1$. The problem of calculating correlation functions of the ground state reduces to counting the number of classically allowed dipole coverings. This counting can be done using row-to-row transfer matrices.

Let T be the transfer matrix for a row of length N_x unit cells. T is a $4^{N_x} \times 4^{N_x}$ matrix and acts on the space of dipole configurations within that row. Note that this Hilbert space includes configurations which are not allowed by the constraint. Such configurations are excluded by setting the corresponding matrix elements of T to zero. The matrix elements of T are either 1 or 0, so that $T_{c',c} = 1$ if the sequence of two row configurations c, c' contains no violations of the constraint, and $T_{c',c} = 0$ otherwise. The dimension of the Hilbert space for a $N_x \times N_y$ lattice with periodic boundary conditions is then given by the trace of powers of the transfer matrix,

$$D_c = \mathrm{Tr}(\mathrm{T}^{\mathrm{N_y}}). \tag{A3}$$

A naive numerical implementation of Eq. (A3) (without using the sparseness of T) gives a complexity of $O(N_y 4^{3N_x})$, compared to going over all the states in the Hilbert space with complexity $O(4^{N_x N_y})$. The values for $N_\pm$ can be similarly found by including projection matrices in the trace, for example

$$N_+ = \mathrm{Tr}\left(T^{N_y - m} P_{p;l} T^m P_{p;0}\right) + \mathrm{Tr}\left(T^{N_y - m} P_{h;l} T^m P_{h;0}\right). \tag{A4}$$

Here $P_{p;l}$ ($P_{h;l}$) is a projection matrix that projects onto configurations which have a particle (a hole) at site $l = 0, 1, \ldots, N_x - 1$ of a given row, respectively. Using this method different correlations for the dipole-directions can also be calculated.

2. Connecting the ground state to a site-factorizable state

In this appendix, we provide evidence that the ground state of H^c_{clock}, Eq. (4.14), is not topologically ordered. To show this, we demonstrate that the ground state of H^c_{clock} can be smoothly connected to the ground state of H_{clock} (without the "hard core" constraint of the dipole-clocks). The ground state of H_{clock} is a site factorizable state, and therefore it is

topologically trivial. The fact that $|\psi_c\rangle$ can be connected to it, while keeping the correlation length finite, is a strong indication that $|\psi_c\rangle$ does not have topological order either. To connect the ground state of $H^c_{\rm clock}$ to the ground state of $H_{\rm clock}$, Eq. (4.11), we define the wave function

$$|\psi(\epsilon)\rangle = \sum_C \epsilon^{n(C)/2} |C\rangle \,. \tag{A5}$$

Here the sum over C runs over all 4^N dipole coverings with one dipole per unit cell, including those which do not respect the constraint. The function $n(\epsilon)$ is an integer counting the number of colliding arrows in configuration C. All allowed configurations M have $n(M) = 0$. Thus changing the value of ϵ interpolates between the ground state of $H^c_{\rm clock}$, $|\psi_c\rangle$, and the ground state of $H_{\rm clock}$, $|\psi_0\rangle$,

$$|\psi(\epsilon = 0)\rangle = |\psi_c\rangle \,, \tag{A6}$$

$$|\psi(\epsilon = 1)\rangle = |\psi_0\rangle \,. \tag{A7}$$

As the density operator $\hat{n}_{(l,m)}$ is still diagonal in the basis of C, we can again use (generalized) transfer matrices to compute density-density correlation functions for any value of ϵ. The result is shown in Fig. 16, and we find no divergence in the correlation length. This supports our conjecture that the ground state $|\psi_c\rangle$ is topologically trivial. Of course, we have not calculated *all* possible correlation functions, so this is an evidence, but not a proof.

To calculate the correlation functions, we make use of equations (A2), (A3), and (A4), with one modification: the transfer matrix $T(\epsilon)$ now depends on the parameter ϵ in the following way

$$(T(\epsilon))_{c',c} = \epsilon^{n(c',c)}, \tag{A8}$$

where $n(c', c)$ is the number of collisions in row-configuration c', plus the number of collisions *between* rows c and c'. The number of collisions in the other row, c, does not come in here, to avoid double counting.

---

[1] M. Greiner, O. Mandel, T. Esslinger, T. W. Hänsch, and I. Bloch, Nature **415**, 39 (2002).

[2] S. Trotzky, P. Cheinet, S. Fölling, M. Feld, U. Schnorrberger, A. M. Rey, A. Polkovnikov, E. A. Demler, M. D. Lukin, and I. Bloch, Science, **319**, 295 (2008).

[3] S. Sachdev, K. Sengupta, and S. M. Girvin, Phys. Rev. B **66**, 075128 (2002).

[4] K. Sengupta, S. Powell, and S. Sachdev, Phys. Rev. A **69**, 053616 (2004).

[5] P. Fendley, K. Sengupta, and S. Sachdev, Phys. Rev. B **69**, 075106 (2004).

[6] Recently, a scheme encoding spin degrees of freedom in position of spinless ultracold fermions has been proposed to simulate field theories: J. I. Cirac, P. Maraner, and J. K. Pachos, Phys. Rev. Lett. **105**, 190403 (2010).

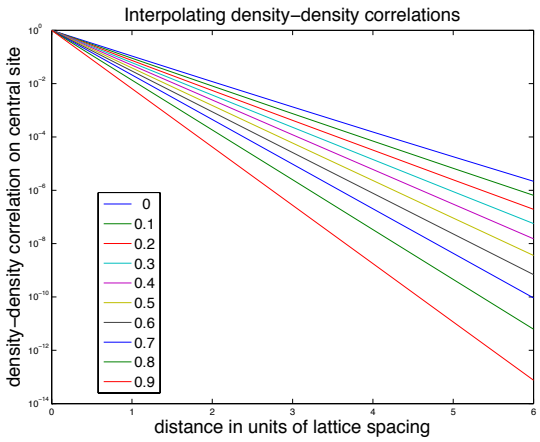

FIG. 16: (Color online) Density-density correlations of a wavefunction which interpolates between the ground states of $H^c_{\rm clock}$ and $H_{\rm clock}$, see text. Different colors stand for different values of the parameter ϵ. The correlation length does not diverge, it decreases as $\epsilon \to 0$. This provides evidence that the state $|\psi_c\rangle$ is topologically trivial.

[7] A two band model for a tilted lattice has been studied in P. Plötz, P. Schlagheck, S. Wimberger, Eur. Phys. J. D (2010), DOI: 10.1140/epjd/e2010-10554-7.

[8] J. Simon, W. S. Bakr, R. Ma, M. E. Tai, P. M. Preiss, and M. Greiner, *Quantum simulation of antiferromagnetic spin chains in an optical lattice*, Nature, doi:10.1038/nature09994 (2011).

[9] D. Jaksch, C. Bruder, J. I. Cirac, C. W. Gardiner, and P. Zoller, Phys. Rev. Lett., **81**, 3108 (1998).

[10] N. Strohmaier, D. Greif, R. Jördens, L. Tarruell, H. Moritz, T. Esslinger, R. Sensarma, D. Pekker, E. Altman, and E. Demler, Phys. Rev. Lett. **104**, 080401 (2010).

[11] T. Kinoshita, T. Wenger, and D. S. Weiss, Science **305**, 1125 (2004).

[12] S. Hofferberth, I. Lesanovsky, B. Fischer, T. Schumm, and J. Schmiedmayer, Nature **449**, 324 (2007).

[13] T. Kitagawa, S. Pielawa, A. Imambekov, J. Schmiedmayer, V. Gritsev, and E. Demler, Phys. Rev. Lett. **104**, 255302 (2010).

[14] For an example of such a non-equilibrium state, see: S. D. Huber and E. Altman, Phys. Rev. B **82**, 184502 (2010).

[15] W. S. Bakr, J. I. Gillen, A. Peng, S. Fölling, and M. Greiner, Nature **462**, 74 (2009).

[16] W. S. Bakr, A. Peng, M. E. Tai, R. Ma, J. Simon, J. I. Gillen, S. Fölling, L. Pollet, and M. Greiner, Science **329**, 547 (2010).

[17] J. F. Sherson, C. Weitenberg, M. Endres, M. Cheneau, I. Bloch, and S. Kuhr, Nature **467**, 68 (2010).

[18] P. R. Johnson, E. Tiesinga, J. V. Porto, and C. J. Williams, New Journal of Physics **11**, 093022 (2009).

[19] S. Will, T. Best, U. Schneider, L. Hackermuller, D.-S. Luhmann, and I. Bloch, Nature **465**

197201 (2010).

[20] W. S. Bakr, private communication.

[21] M. A. Novotny and D. P. Landau, J. Mag. and Mag. Mat. **54-57**, 685 (1986).

[22] A. A. Ovchinnikov, D. V. Dmitriev, V. Ya. Krivnov, and V. O. Cheranovskii, Phys. Rev. B **68**, 214406 (2003).

[23] It is worth noting here that these effective Hamiltonians always have full translational symmetry both parallel and transverse to the tilt directions, unlike Eq. (1.1c) which is only invariant under translations transverse to the tilt. Of course, there is no equivalence between the physics parallel and transverse to the tilt direction, and the lattice rotation symmetry is reduced by the tilt, even in the effective Hamiltonian.

[24] D. S. Rokhsar and S. A. Kivelson, Phys. Rev. Lett. **61**, 2376 (1988).

[25] O. Perron, *Zur Theorie der Matrices*, Mathematische Annalen 64 (2): 248263 (1907).

[26] G. Frobenius, *Über Matrizen aus nicht negativen Elementen*, Sitzungsber. Königl. Preuss. Akad. Wiss.: 456477 (1912).

[27] A. Auerbach, *Interacting Electrons and Quantum Magnetism*, Springer (1994).

[28] K. S. Raman, R. Moessner and S. L. Sondhi, Phys. Rev. B **72**, 064413 (2005).

[29] R. J. Baxter, *Exactly solved models in statistical mechanics*, Academic Press (1982).

[30] N. Read and S. Sachdev, Phys. Rev. B **42**, 4568 (1990).

[31] A. Vishwanath, L. Balents, and T. Senthil, Phys. Rev. B **69**, 224416 (2004).

[32] E. Fradkin, D. A. Huse, R. Moessner, V. Oganesyan, and S. L. Sondhi, Phys. Rev. B **69**, 224415 (2004).

[33] P. W. Leung, K. C. Chiu, and K. J. Runge, Phys. Rev. B **54**, 12938 (1996).

[34] O. F Syljuåsen, Phys. Rev. B, **73**, 245105 (2006).

[35] A. Ralko, D. Poilblanc, and R. Moessner, Phys. Rev. Lett.,**100**, 037201 (2008).

[36] E. Fradkin and S. A. Kivelson, Mod. Phys. Lett. B **4**, 225 (1990).

[37] L. Balents, L. Bartosch, A. Burkov, S. Sachdev, and K. Sengupta, Phys. Rev. B **71**, 144509 (2005).

[38] L. Tonks, Phys. Rev. **50**, 955 (1936); M. Girardeau, J. Math. Phys. **1**, 516 (1960).

[39] V. J. Emery, E. Fradkin, S. A. Kivelson, and T. C. Lubensky, Phys. Rev. Lett. **85**, 2160 (2000).

[40] A. Vishwanath and D. Carpentier, Phys. Rev. Lett. **86**, 676 (2001).